Available online at www.sciencedirect.com
SCIENCE DIRECT®

Journal of the European Ceramic Society 23 (2003) 3097–3103

www.elsevier.com/locate/jeurceramsoc

Alterations in cordierite based burners subjected to radiant mode ageing conditions

E. García, P. Miranzo, M.I. Osendi*

Instituto de Cerámica y Vidrio, CSIC. 28049 Cantoblanco, Madrid, Spain

Received 24 June 2002; received in revised form 30 January 2003; accepted 8 February 2003

Abstract

Industrially developed perforated cordierite ceramic tiles were aged under accelerated conditions in a radiant combustion mode. Changes in the original phases, microstructure and mechanical properties were evidenced in the aged plates. The extent of the degraded zone was localized at the uppermost layer of the burner. These effects are attributed to corrosion of the cordierite-based material by gaseous species generated in the combustion.

Keywords: Burners; Cordierite; Corrosion; Aging

1. Introduction

The CO_x, NO_x and SO_x emissions generated by the combustion of fossil fuels contribute highly to environmental degradation. These emissions can be eliminated (SO_x) or partially reduced (CO_x, NO_x) by using gas burners of improved combustion efficiency and by working at lower flame temperatures.[1] In this sense, infrared radiant burners seem to be an efficient and clean way to get energy from natural gas.[2] Both metals and ceramics are used for radiant burner applications in many shapes and configurations, such as, perforated plates, foams or fibermats.[3]

The flame temperature drops as the energy is absorbed by the ceramic component and a balance is created among the temperatures of the flame, of the ceramics and of the hot gases. Here, we will focus on perforated ceramic plates, which typically have several thousands of closely packed channels through which gas flows. A high porosity in the material is desirable in order to improve the combustion performance[4] and to reduce the thermal conductivity of the plate. Initially, porous cordierite seem to be a suitable material for this application due to its low thermal conductivity[5] and low thermal expansion coefficient[6] that enhance its thermal shock response.[7]

In a radiant combustion mode, the flame temperature together with the concentration of transitory chemical species, like OH and H, have been proposed by Lannutti et al.[8,9] as the responsible agents for degradation of different ceramic plates. In fact, it was assumed that the degradation kinetics of ceramic burners was governed by the local concentration of monatomic hydrogen, as being the most harmful species.[9] Concentrations of such gases increased monotonically with the combustion temperature. Model calculations for porous ceramic plates[10] revealed maximum concentration of H, O and OH at a short distance (300–500 μm) outside the burner surface, although these species can penetrate up to 200 μm inside the burner.

Depending on the experimental assumptions, molar fractions of H between 10^{-8} and 2×10^{-4} were determined for a burner surface temperature of 1100 K.[8,10] Even though these concentrations are very low, they are very important owing to the fact that volatile hydroxides or suboxides can form by reaction of the ceramic with the monatomic hydrogen.[8,9]

Consequently, cordierite perforated plates were tested in the radiant mode as being the most aggressive working condition. The plates aged in that way were analyzed to correlate the total combustion time to possible variations in the plate properties with the aim of finding

* Corresponding autor. Tel.: +34-91-735-5868; fax: +34-9-735-5843.
E-mail address: miosendi@icv.csic.es (M.I. Osendi).

0955-2219/03/$ - see front matter © 2003 Elsevier Ltd. All rights reserved.
doi:10.1016/S0955-2219(03)00093-1

a convenient parameter for monitoring the burner degradation. The degradation of these perforated ceramic tiles is experimentally proved and treated according to the above corrosion model.

2. Experimental

The perforated ceramic tiles, developed by Morgan Matroc (Barcelona, Spain),[a] had a rectangular shape (13×16×1.5 cm) with thousands of cylindrical evenly arranged through thickness holes. Two types of plates were studied, named P-1 and P-2. Both plates were alike except by the hole diameter, which was 1.29 mm for the P-1 plates and 1.0 mm for the P-2 (Fig. 1).

The apparent density (ρ) of both kinds of plates, measured by the water immersion technique, was approximately 0.60 g/cm^3 and the porosity was around 70 vol.% in both. Plates had a chemical composition close to stoichiometric cordierite ($2MgO{\cdot}2Al_2O_3{\cdot}5SiO_2$) and presented iron and titanium oxides as the main impurities, each below 1 wt.%. The X-ray diffraction (XRD) patterns recorded from powdered samples showed the presence of indialite, which is the hexagonal form of cordierite, as the main phase together with traces of mullite.

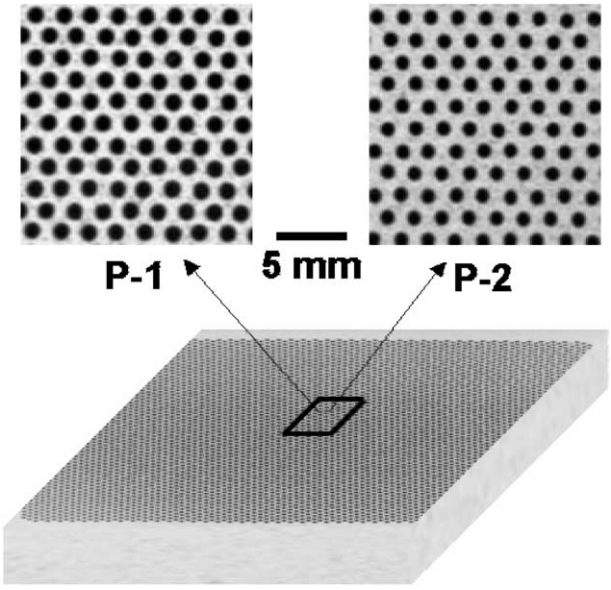

Fig. 1. Drawing of the typical plate geometry of both plates with a higher magnification top view of both plates: type P-1 (left) and type P-2 (right).

[a] Task accomplished within the Lifeburn project (III Brite-Euram Framework). Partners to the project were N.V. Acotech, CATIM S.A, CSIC-ICV, EcoCeramics B.V, Eindhoven University of Technology, Gaz de France, Ikerlan, INETI, Italgas, Kanthal AB, Morgan Matroc, N.V. Nederlandse, Politecnico di Torino, Repsol Petroleo S.A. and Worgas Bruciatori.

Both types of plate were aged in Standardised Combustion Chambers (SCC) developed[a] by Ikerlan S. A. (Vitoria, Spain) using natural gas as fuel. These combustion chambers consisted basically in a combustor and a control system, which allowed an automatic control of the combustion parameters. The combustor can reproduce the usual operating conditions existing in commercial boliers used for espace heating. The gas and the air were mixed in a prechamber before passing along the ceramic plate channels and reaching the top of the plates where the mixture was ignited. Two walls of the combustion chamber had windows that allowed the visual observation of the combustion. The temperature and other combustion parameters (concentration of O_2, CO_x and NO_x, pressure drop etc.) were measured by different sensors located in specific points of the chamber and registered by the control system.

Ageing tests carried out in these combustion chambers were on/off cycles whose duration varied from 75 to 3600 s. The maximum ageing time tested was 3000 h of radiant mode working. The plates were removed after a fixed number of cycles for examination of their properties, phases and microstructure.

The elastic modulus of aged plates was determined by the resonance frequency method. Measurements were done on the whole plate using a bending configuration and were averaged over two plates. For strength measurements, bars of dimensions 13×15×130, in mm, were machined from the original and aged plates and tested in three-point bending, with a span of 80 mm and a cross-speed head of 0.5 mm min^{-1}. The traction surface of the test bars was always the corresponding radiant surface. At least 6 bars were tested for each condition.

For the microstructure observations, the top (combustion) surface and cross-section specimens (Fig. 2) of both aged and original plates were gold coated before

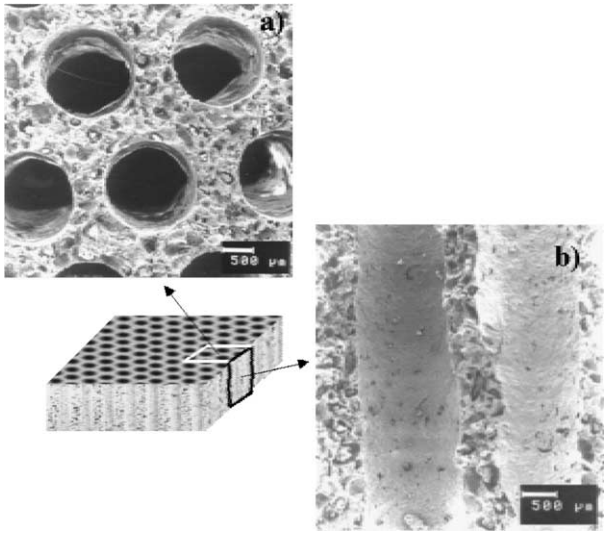

Fig. 2. Examples of the structure of the top combustion surface (a) and the cross section (b) of a plate.

being examined by scanning electron microscope (SEM). Standardless microanalyses were done by energy dispersive X-ray spectroscopy (EDS) in selected zones along the gas channels using a window analysis of 50×50 μm^2.

XRD patterns were taken at a fixed incident angle of 0.5° to reduce the penetration depth of the X-ray beam, which made it possible to analyse only the surface layer. The X-ray penetration depth in a cordierite material for the 0.5° scanning condition was estimated as ≈1 μm.[11] Specimens were sectioned from aged plates and mounted in the XRD holder with the scanned surface as the combustion one. Once the pattern was recorded, the surface was removed by gently grinding and the thickness reduction measured with a micrometer with an accuracy of ±0.001 mm. This process was stepwise repeated until the initial composition of the plate was reached.

3. Results and discussion

Elastic modulus values are represented versus total ageing time, considered as the total time at the maximum temperature, in Fig. 3 for both materials. Despite the dispersion in the data, the trend lines give a fair idea of the time evolution in both plates. A clear reduction in elastic modulus (74%) with total ageing time is appreciable for the P-1 plate, while in the P-2 plate it is not perceptible. This reduction can be caused by an increase in porosity and/or the presence of cracks. Therefore, the decrease in elastic modulus of P-1 compared to P-2 indicates larger defects in the former plates when aged.

Corresponding bending strength values vs. ageing time are depicted in Fig. 4. There is a reduction of bending strength with total burning time for both plates that is again larger for the P-1 (90%) than for the P-2 (25%) plates. Accordingly, flaw sizes seem to increase

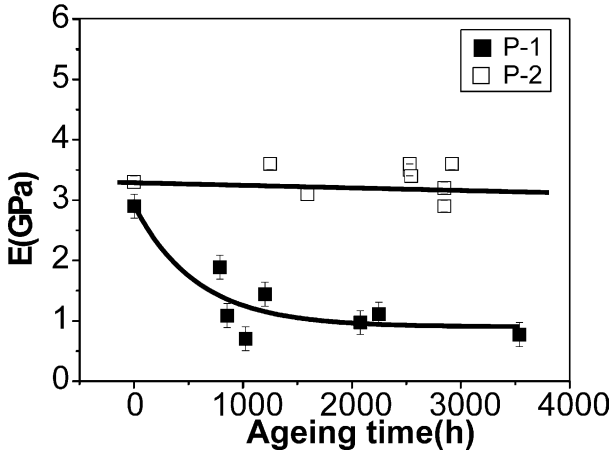

Fig. 3. Elastic modulus vs. ageing time in a radiant combustion mode for P-1 and P-2 plates.

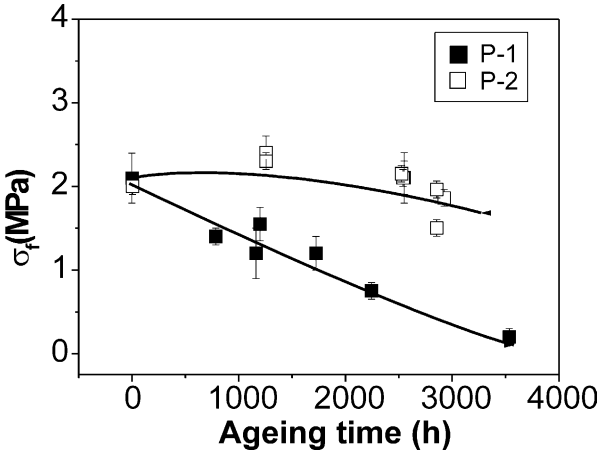

Fig. 4. Bending strength vs. ageing time in a radiant combustion mode for P-1 and P-2 plates.

faster with ageing time in the P-1 plates, although a decrease in their toughness cannot be excluded.

In Fig. 5, some examples of the microstructures observed in the original and aged plates near the combustion face are compared. No difference will be made between P1 and P-2 plates as both presented the same features. It is noticeable that a glassy phase usually surrounds grains in the unburned plate (Fig. 5a) and it is lacking in the aged plates, where the microstructures are more precisely revealed (Fig. 5b–d). Fig. 5b and c show typical features found near the combustion face, where flake-like structures (marked as "f" in Fig. 5b) and worn down grains (marked as "w" in Fig. 5c) indicate that corrosion has occurred. Fig. 5d corresponds to an area just below the combustion face that has small acicular grains of mullite (marked as "m" in Fig. 5d) surrounding the larger cordierite crystals (marked as "c" in Fig. 5d). Both phases were identified by EDS point analyses done in each area. Microstructure shown in Fig. 5d is probably close to the original microstructure of the plates that now is perfectly revealed because the glass phase is absent. These porous corroded microstructures shown in Fig. 5b and c are responsible for the loss in elastic modulus and bending strength of the aged plates (Figs. 3 and 4).

Certain evidence of changes in the average composition across the aged plates is confirmed by the EDS window analysis done along a gas channel, from the combustion face down to the cooler face. To show it, contents of SiO_2, Al_2O_3 and MgO in different zones that correspond to increasing depths along a gas channel are plotted in Fig. 6. It is obvious that the percentage of SiO_2 decreases drastically at the uppermost surface compared to the level of the plate inner areas. This result totally agrees with above microstructural observations that showed the loss of the original glassy phase. The average EDS window analysis for inner areas (53.1 SiO_2 wt.%, 35.8 Al_2O_3 wt.% 11.1 MgO wt.%) give a

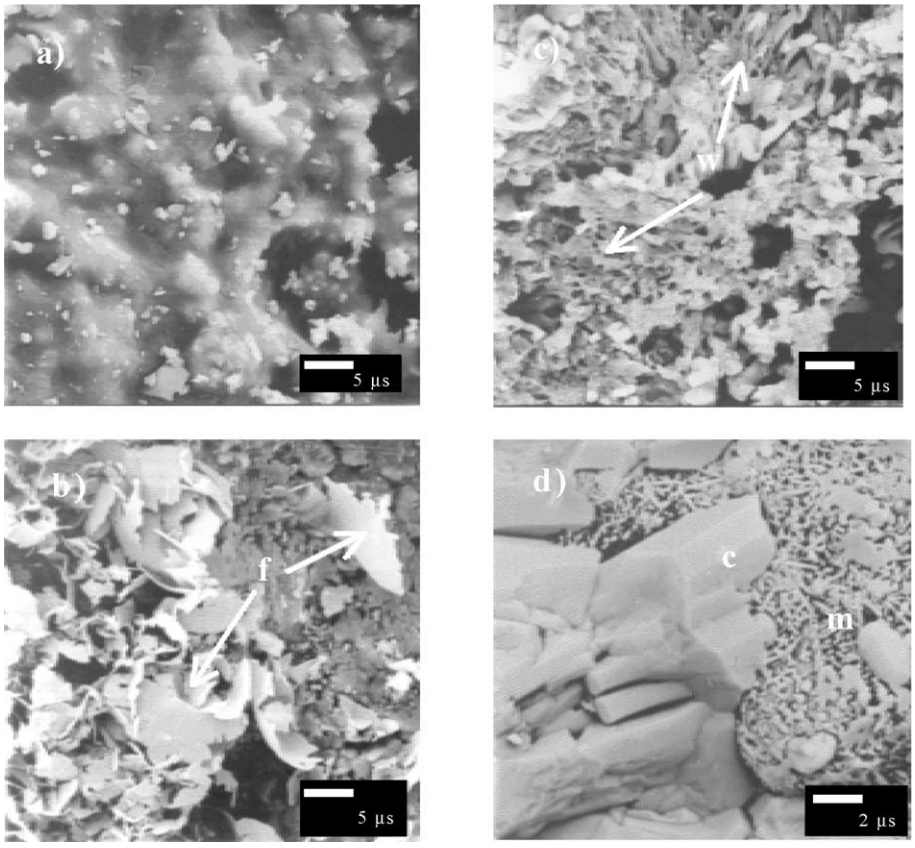

Fig. 5. Representative SEM micrographs of specimens from different zones: (a) gas channel region in an original P-1 plate, (b) gas channel zone near the combustion surface in a P-2 plate aged for 2500 h where "f" indicates the flake type grains, (c) gas channel zone near the combustion surface in a P-1 plate aged 1177 h ("w" indicates the worn out grains) and d) region below that shown in (b) for the same specimen (i.e., further from the combustion surface), where "c" and "m" refer to cordierite and mullite crystals respectively.

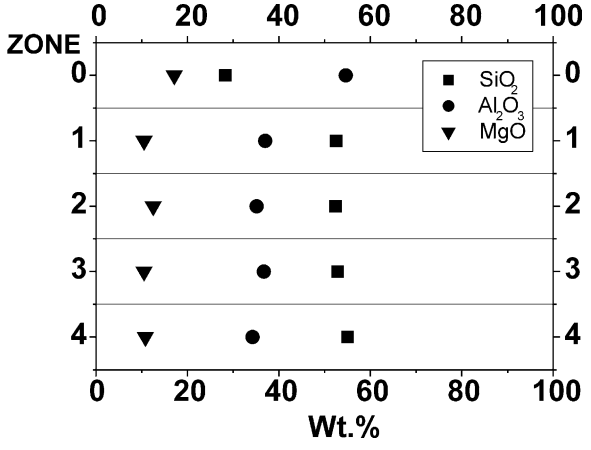

Fig. 6. EDS window microanalyses along a gas channel cross-section of an aged (2500 h) P-2 plate. Each zone corresponds to a different depth along the surface channel: the combustion upper layer (zone 0), intermediate plate region (zones 1–3) and the cool zone at the bottom of the plate (zone 4).

composition quite close to the chemical analyses of the original plates (51.4 wt.% SiO_2, 34.79 Al_2O_3 wt.% 13.81 MgO wt.%), considering that the analyses were standardless. Both analyses were used to get some weight factors (0.97 for SiO_2 and Al_2O_3, and 1.25 for MgO) that correct the EDS analysis, which basically underestimates the MgO content.

Furthermore, this change in chemical composition at the upper surface was accompanied by a change in the original phases as Fig. 7 demonstrates. In the figure, a selection of XRD patterns recorded from a P-2 specimen aged for 2540 h at increased depths from the combustion face are displayed. At the combustion surface, the peaks of indialite, together with some peaks characteristic of spinel (MgO. Al_2O_3) and forsterite (2MgO. SiO_2) can be observed. The spinel and forsterite peaks gradually reduce their intensity in the patterns of the plate inner regions. The original pattern of the cordierite plates is recovered after removing about 150 μm in depth from the top surface layer of the 2540 h aged plate. A similar evolution of phases was observed for the longer time aged P-1 plates.

If we correct the average EDS composition of aged plates at the top layer by the above weight factors, the composition (27 wt.% SiO_2, 52 wt.% Al_2O_3 and 21 wt.% MgO) will shift to the primary crystallisation field of spinel according to the MgO–Al_2O_3–SiO_2 phase equilibrium diagram.[12] The compatible phases for this

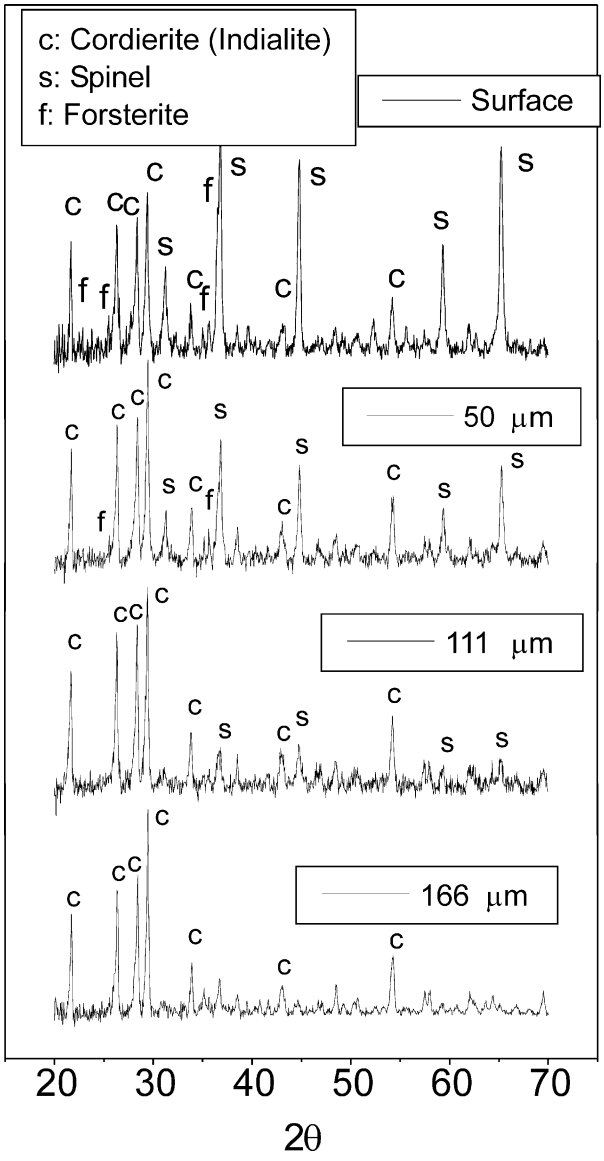

Fig. 7. Grazing angle XRD spectra of a P-2 plate aged for 2520 h recorded at different depths from the combustion surface.

composition are cordierite, spinel and forsterite, as shown in Fig. 8, which totally agrees with the experimental observations given by the XRD for the uppermost layer (see Fig. 7).

The combustion environment (high temperatures and presence of radicals) is directly related to the plate degradation. Among the oxide ceramics, silica and silica-containing materials show a poor stability in reducing atmospheres.[8] Particularly, silica can be reduced by monatomic hydrogen according to the expression.[8,9]

$$SiO_2 + 2H(g) = SiO(g) + H_2O(g) \quad (1)$$

In a similar way, we can formulate reactions for the decomposition of cordierite by pure monatomic dry hydrogen:

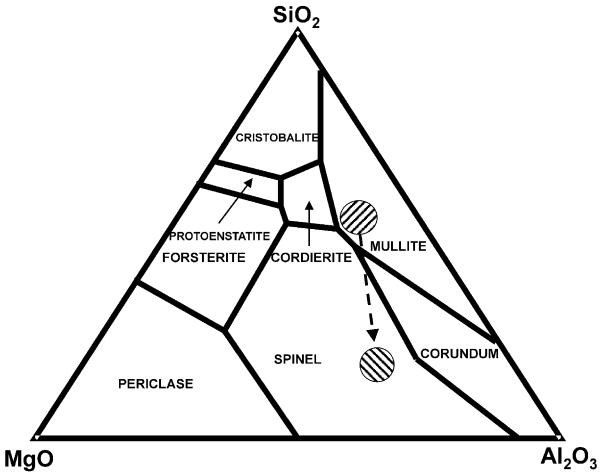

Fig. 8. Scheme of $MgO–Al_2O_3–SiO_2$ phase equilibrium diagram [12] showing the shift in the average composition (shaded circle) of the degraded layer at the combustion surface as estimated by the microanalysis.

$$2MgO\cdot 2Al_2O_3\cdot 5SiO_2 + 10H(g) \underset{\text{cordierite}}{} = 2MgO + 2Al_2O_3 + 5SiO(g) + 5H_2O(g) \quad (2)$$

$$2MgO\cdot 2Al_2O_3\cdot 5SiO_2 + 10H(g) \underset{\text{cordierite}}{} = 2\left(\underset{\text{spinel}}{MgO\cdot Al_2O_3}\right) + 5SiO(g) + 5H_2O(g) \quad (3)$$

In the second reaction, spinel formation is assumed because it is experimentally observed in the degraded zone (Fig. 7). Forsterite has not been introduced in the reaction because of the small amount formed.

We have calculated the Gibbs free energy per mol of monatomic hydrogen for both reactions, using tabulated thermodynamic data. Results are plotted as a function of temperature in Fig. 9, together with the analogous data for silica reduction [Eq. (1)]. The figure shows that the decomposition of cordierite to form spinel is favourable for temperatures of 900 °C or above, which is within the typical range of surface temperatures of the burner rig working in radiant mode.[13] The above thermodynamic calculations confirm that, in the presence of monatomic hydrogen, the decomposition of cordierite to form spinel is the most favourable reaction as observed after the removal of the glassy phase covering the grains.

The extension of this corrosion zone is limited to the near surface region (Figs. 5–7), which is explained by two reasons, first, the rapid temperature drop occurring within the burner plate[13] and second, the concentration of the free radicals at the combustion surface.[10] An additional experimental confirmation of this localised degradation is offered in Fig. 10. This figure collects values for the elastic modulus of several aged plates as a function of the thickness of the layer removed from the

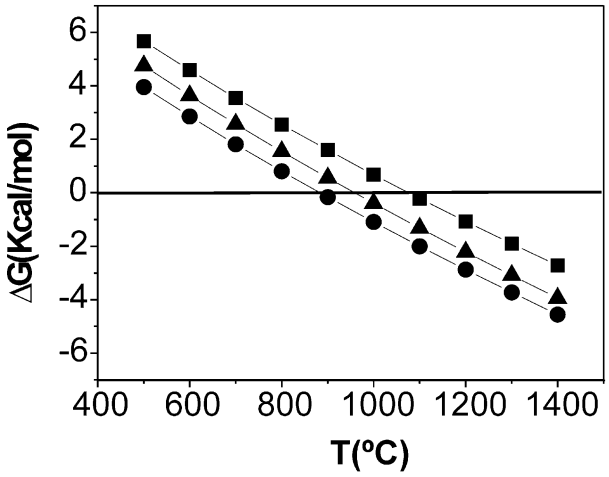

Fig. 9. Gibbs free energy for the different cordierite decomposition reactions per mol of monatomic hydrogen. Squares correspond to the reduction of cordierite into alumina and silica, circles represent the decomposition reaction to give spinel. The data for the decomposition of silica is also plotted for comparison (triangles).

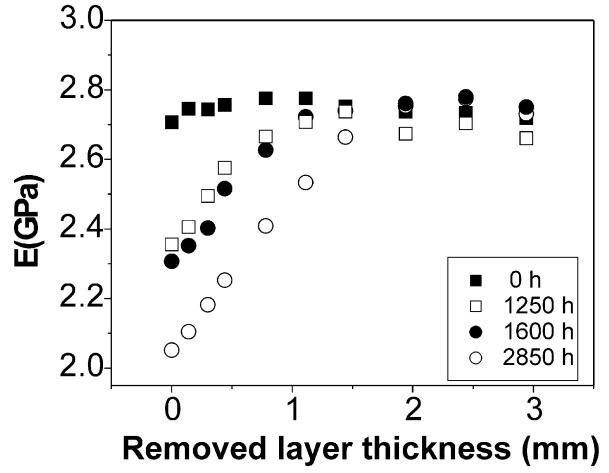

Fig. 10. Elastic modulus of prismatic bars machined from different P-2 aged plates as a function of the removed surface layer thickness (combustion surface). The values measured for an original plate following the same procedure are also given for comparison. Ageing times are indicated in the legend.

combustion surface by gently polishing. Measurements were done on bars (13×20×60 in mm) machined from the aged plates and subjected to stepwise polishing repeated until steady values were reached. In the plot, a distinct gradual recovering of the elastic modulus in aged P-2 plates by the progressive removal of material from the combustion face is observed for different ageing times. The same procedure was followed for an original plate, to demonstrate that it was not an effect of the change in the geometry of the test bars, as it is seen in Fig. 10. Considering these tests and the XRD results, we can say that the extension of the corrosion zone is in the range of 100–1500 μm for ageing times around 3000 h. This range depends logically on the technique considered to evaluate it; in the sense that original crystalline phases are recuperated after a 100 μm layer is removed, while the original flaw population is regained only when a layer of approx. 1mm is eliminated. Therefore, the decrease in the elastic modulus and consequently, in strength, observed in aged plates is associated with the localised corrosion mechanism described.

Kinetic effects linked to the size of the gas channels can explain the different decay rates of both E and σ_F between P-1 and P-2 plates (Figs. 3 and 4), although they show same corrosion mechanism. It is known that hole size determines the gas speed and therefore the distance where the flame front stabilises.[13] For bigger channel diameters the flame front is closer to burner surface and higher temperatures are therefore reached at the top layer, which accelerates the degradation effects.

4. Conclusions

Cordierite based plates aged in a combustion radiant mode show a monotonous decrease in both elastic modulus and bending strength with ageing time. Both properties are effective parameters to check the degradation extent.

Localised degradation at the combustion face in cordierite-based ceramic plates occurs by both the removal of the protective glassy phase and simultaneous decomposition of cordierite by monatomic hydrogen. The reduction reaction of cordierite during the combustion to form spinel is thermodynamically more favourable in complete consonance with the experimental data. This reaction is limited to a small zone close to the radiant surface, where the burner temperatures are higher and where a low but meaningful concentration of radicals can be assumed. Reducing the diameter of the gas channels can retard this effect.

Acknowledgements

This project has been founded by the EC (Brite-EURAM III Program) under contract BR-CT98-0743 (LIFEBURN Project). Part of the work was also supported by the Ministery of Science and Technology (Spain) under the project MAT1999-0168-CE.

References

1. Bouma, P. H. and De Goey, L. P. H., Premixed combustion on ceramic foam burners. *Combust. Flame*, 1999, **119**, 133–143.
2. Ticó, L., Infrared—clean and efficient heat at the speed of light. *Global Ceramic Review*, 1998, **99**(4), 12–13.
3. Kilham, J. K. and Laningan, E. P., A study of the mechanism of radiant burners. *Institution of Gas Engineers Journal*, 1970, **10**, 700–713.

4. Abe, F., Hasewaga, H., Fujita, T. and Maeda, M., High Temperature Surface Combustion Burner, US Patent Na. 4673349, 6/1987.
5. Cabannes, F. and Minges, M. L., Thermal conductivity and thermal diffusivity of a cordierite-based ceramic. *Results of a CODATA measurement program. High Temp. - High Press.*, 1989, **21**, 69–78.
6. Lachman, I. M., Bagley, R. D. and Lewis, R. M., Thermal expansion of extruded cordierite ceramics. *Ceram. Bull.*, 1981, **60**, 202–205.
7. ZhiQin, B. and JieYao, L., Cordierite honeycomb ceramic for exhaust purifier application. In *Proceedings of the Third European Ceramic Society Meeting*, ed. P. Durán and J. F. Fernandez. Faenza Editrice Ibérica, Madrid, 1993, pp. 1103–1106.
8. Lannutti, J. L. and Rapp, R. A., *Degradation of Radiant Ceramics Structures in Combustion Atmospheres*. GRI-reports 92/0408, 1992 and 93/0435 1994.
9. Wang, G. and Lannutti, J. L., Surface cavity microenvironments in a porous ceramic radiant burner. *Combust. Sci. Technol.*, 1994, **95**, 277–311.
10. Bouma, P. H., Premixed combustion on ceramic foam burners. Lifeburn Project. *Deliverable*, 2001, **57**.
11. Levin, L. S. and Kimmel, G., *Quantitative X-ray Diffractometry*. Springer - Verlag, New York, 1995.
12. Schreyer, W. and y Schairer, J. F., Composition and structural states of anhydrous Mg-cordierites: a re-investigation of the system $MgO–Al_2O_3–SiO_3$. *J. Petrol.*, 1961, **2**, 324–406.
13. Final public report of the *Lifeburn* Project, Date of issue 5 March 2002.